Degradability of unpaved roads submitted to traffic and environmental solicitations: laboratory scale

O. Sediki & A.R. Razakamanantsoa
Institut Français des Sciences et Technologies des Transports, de l'Aménagement et des Réseaux GERS-GMG
O. Sediki & M. Hattab
Laboratoire d'Etude des Microstructures et de Mécanique des Matériaux, Université de Lorraine CNRS UMR 7239
T. Le Borgne
Bouygues – Travaux Publics
J-M. Fleureau
Université Paris Saclay, CentraleSupélec MSSMat CNRS UMR 8579
P. Gotteland
Fédération Nationale des Travaux Publics

ABSTRACT: Dust emission generated during earthwork induces security nuisances for workers, residents and other activities around the site. At present, dust abatement is mainly done by water spraying. Since water spraying is not environmentally friendly, it becomes an economic and ecological challenge for companies. To enhance water saving, analysis of the mechanism of dust production is fundamental. This study aims to analyse the combined effects of traffic cycles and hydromechanical stresses on surface erosion and the modification of the microstructure of compacted soils. Roller compaction and traffic cycles were carried out in the laboratory on two soils composed by mixtures of Speswhite kaolin clay and Hostun sand, submitted to different hydric states and compaction degrees. Test results underline that the soil degradation under traffic cycles is governed by the compaction configuration. The grain size distribution of eroded particles features aggregates coarser than in the reference soil. Traffic cycles and compaction modify the soil microstructure. A decrease in the macro-pore size is measured for all the tested compaction configurations. However, combination of traffic cycles and drying presents a less significant effect on the decrease of the macro-pore sizes.

1 INTRODUCTION

The fugitive dust generated during traffic on unpaved roads affects the roadside safety and the environment (Edvardsson & Magnusson 2009). Fugitive dust might impair visibility and dust particles can be deposited on buildings, plant leaves and can cause excessive wear to passing vehicles (Addo & Sanders 1995).

Boulter (2005) stated that particulate matter smaller than 10 μm (PM10) impairs visibility. Loss of visibility is due to the light scattering from fine and coarse particles fractions (Moosmuller et al. 2005). Dust emission is significantly generated by the erosion of aggregates during traffic cycles (Lohnes & Corree 2002). The mechanism of airborne dust emission is well developed in the literature (Vinkovic 2005; Han et al. 2009) whereas, the mechanism of dust production remains unknown.

Some recent studies analysed the effect of several primary factors on dust production in the case of unpaved road (Bolander & Yamada 1999; Foley & Cropley 1996; Addo & Sanders 1995; Etymezian et al. 2003; Thenoux et al. 2007).

Bolander and Yamada (1999) stated that dust abatement could be done in several ways: agglomeration of fines particles, increase of the adherence of particles on the soil surface, or increase of the density of road surface material. According to Thenoux et al. (2007), unpaved road construction can be improved by increasing the soil homogeneity and compaction quality.

A change in practice during earthworks is also proposed. Succarieh (1992) recommended reduction of vehicle speed, while, Moses et al. (2012) concluded that reduction of traffic volume significantly contributes to dust reduction. Some other setting parameters are proposed in the literature such as- fiberglass or granular matter covering. These solutions remain suitable in the short term but still uneconomic.

At present, dust reduction is done mainly by water spraying, but such procedure is not environmentally friendly. To enhance water saving, analysis of the mechanism of dust production is fundamental.

This study aims to analyse the combined effect of traffic cycles and hydromechanics stresses on surface degradability, and the modification of the microstructure of compacted soils.

2 MATERIALS AND METHODS

2.1 *Experimental procedure*

Soil compaction and traffic cycles were carried out by means of a laboratory roller compactor and a laboratory traffic simulator, respectively. Before traffic test, soil specimens were prepared and compacted at w_{SPO}

and 0.75w_{SPO} and dry unit weights of γ_{dSPO} and γ_{d1} (Fig. 1).

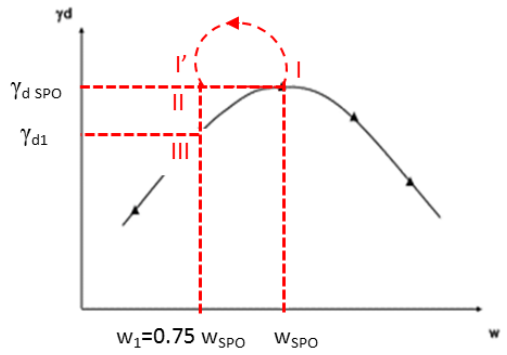

Figure 1. Scheme of tested configurations.

Specimen prepared under configuration I is dried after compaction down to a hydric state of 0.75 of Standard Proctor Optimum (SPO) water content (0.75 w_{SPO}) to obtain I', while specimens compacted under configurations II and III are submitted to traffic cycles directly after compaction. Details of prepared specimens before degradation tests are summarized in Table 1.

Table 1. Characteristics of tested configurations.

	Config.	Compaction conditions	Drying	Degradation conditions
Rolling	I	w_{SPO} / γ_{dSPO}	No	w_{SPO} / γ_{dSPO}
	II	0.75w_{SPO} / γ_{dSPO}	No	0.75w_{SPO} / γ_{dSPO}
	III	0.75w_{SPO} / γ_{d1}	No	0.75w_{SPO} / γ_{d1}
Drying + Rolling	I'	w_{SPO} / γ_{dSPO}	Yes	0.75w_{SPO} / γ_{dSPO}

Test configurations I, II, and III are used to highlight the influence of compaction, while, I and I' are used to clarify the influence of drying.

The tests were performed on two soils composed by mixtures of Speswhite kaolin clay and Hostun sand. The loss of mass, the change in the grain size distribution between eroded soil particles and soil reference and the evolution of the Pore Size Distribution (PSD) of the compacted soil, resulting from the traffic cycles, were analysed. Reference soil corresponds to the unconsolidated dry soil.

2.2 *Soil properties*

The two fine-grained soils are formed by mixtures of sand from Hostun HN38 and kaolin Speswhite clay: the first mixture is composed by 50% of both sand and clay soils (noted S50K50) and the second is composed by 75% of sand HN38 and 25% of Speswhite kaolin clay (noted S75K25). Speswhite kaolin clay is used as reference for compaction and shear tests. The Standard Normal Proctor compaction curves of the tested soils are shown in Figure 2. The geotechnical properties of the tested soils are summarized in Table 2. The measured grain size characteristics and physical properties are used to establish the soils classification according to American Association of State Highway and Transportation Officials (AASHTO) Standards.

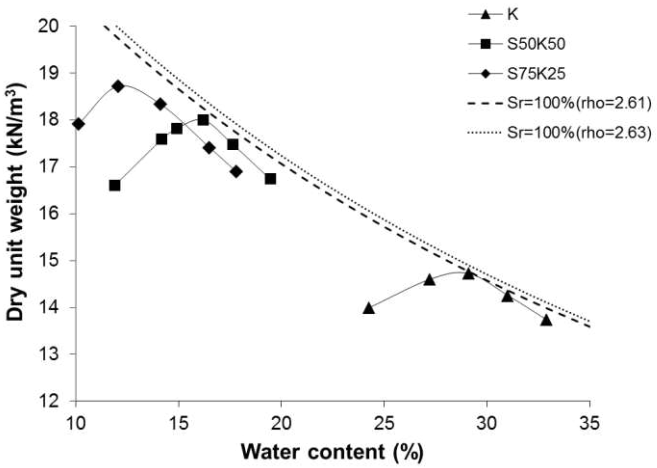

Figure 2. Normal Proctor compaction curves of tested soils.

Table 2. Geotechnical soil properties.

	K	Mixture S50K50	Mixture S75K25
Grain size characteristics			
D10 (µm)	1.1	1.5	2.5
Dmax (µm)	160	500	500
Coefficient of curvature	1.2	0.70	0.48
Coefficient of uniformity	5.1	9.56	46.26
Physical properties			
Liquid limit (%)	55.0	29.9	23.1
Plastocity Index (%)	25.0	12.62	7.57
Methylene Blue Value (g/100g)	1.56	0.74	0.43
Specific gravity	2.62	2.61	2.63
Standard compaction tests			
w_{SPO} (%)	28.2	16.0	12.4
γ_{dSPO} (kN/m^3)	14.70	18.01	18.73
AASHTO Classification (ASTM D2487-85)	A-6	A-6	A-4

2.3 *Experimental programme*

2.3.1 *Soil preparation procedure*

Unconsolidated soils were oven-dried at 40°C during 48 hr, prior to mixing to form the mixtures S50K50 and S75K25. Homogenised dry soils were wetted using tap water up to w_{SPO} and 0.75 w_{SPO}. Prepared soils are put into sealed bags for at least 24 hr for hydric homogenization.

2.3.2 *Shear tests*

Shear characteristics of tested soils are measured to deduce the cohesion (adherence) and the friction angle of soil. The shear characteristics of tested soils are

determined using the Direct Shear Test (DST) according to French Standard NF P 94-071. Shear tests are carried out on statically compacted cylindrical specimens of 60 mm in diameter and 35 mm in height. The specimens are compacted to the SPO dry unit weight γ_{dSPO} at w_{SPO} of each tested soil. All tests were carried out using a Standard DST apparatus under three normal loads of 1.08 KN, 2.16 KN and 3.14 KN, corresponding to three usual roller compaction engines (Dynapac CA1300D, XS-Series Road roller XS122, and BOMAG BW 219 PDH-4, respectively). Each shear test series is duplicated. A total of 12 shear tests was carried out in this study.

2.3.3 *Roller compaction*

Prior to traffic cycles, specimens of 500*180*50 mm^3 are prepared by compaction in the laboratory using a laboratory roller compactor. The laboratory roller compactor allows applying continuous stress tensor rotation on the soil similar to that observed in the field. Compaction effort used for the study corresponds to Bomag BW 219 PDH-4. This value is equal to 10.50 KN. Eight compacted specimens were made for the present study.

2.3.4 *Degradation test*

Traffic tests are performed to assess the potential of erosion of the compacted soil by means of the Laboratory Traffic Simulator (LTS) shown in Figure 3. The LTS is composed of a solid base, on which the specimen is kept and a pneumatic tire inflated at $6*10^5$ Pa. Both base and tire are related to a command table. The latter allows to adjust the number of cycles, the wheel velocity and the vertical weight *i.e.* traffic pressure. In this study, the number of cycles is fixed at 10 000 cycles, which corresponds to the daily number of cycles for an unpaved road. The wheel frequency is adjusted at 1 Hz, *i.e.* 3.6 km/h, which corresponds to the maximum velocity that the device can provide. The applied vertical effort is equal to $3.2*10^5$ kPa. This value corresponds to the weight of an empty dumper.

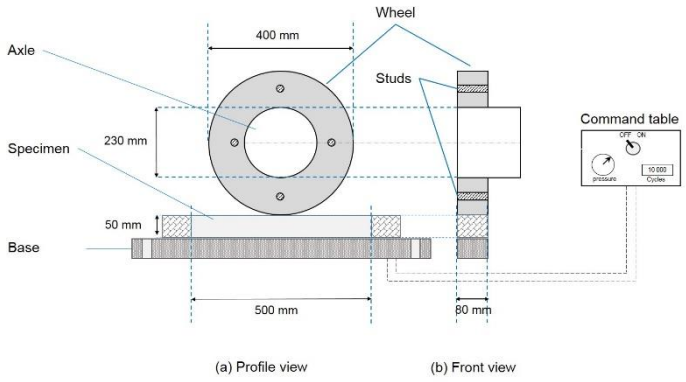

Figure 3. Scheme of Laboratory Traffic Simulator (LTS).

After adjusting the wheel velocity, the vertical pressure and number of cycles, the compacted specimen is subjected to a traffic cycles.

At the end of the test, several parameters are measured:

- The eroded mass collected at the soil surface by means of soft manual brush. A special care is taken to avoid an additional damage at the soil surface;
- The grain size distribution of the eroded soil, was measured using a laser granulometer Malvern Mastersizer 3000;
- The Pore Size Distribution (PSD) of the soil submitted to traffic cycles, sampled at the core of the specimens. PSD measurements are done using a Mercury Intrusion Porosimetry (MIP) method by a Micromeritics AutoPore IV-9500 porosimeter.

3 RESULTS AND DISCUSSIONS

3.1 *Shear strength results*

Figure 4 shows typical shear stress – normal stress curves for the studied soils. Mechanical properties such as cohesion and friction angle are also mentioned in Figure 4.

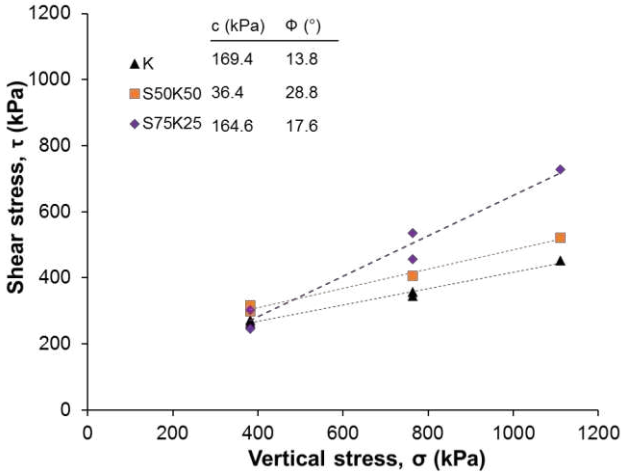

Figure 4. Results of direct shear tests of studied soils.

Results show that the shear stress measured for S75K25 is higher than that of S50K50 under high stresses, whereas S75K25 presents a lower value of cohesion compared to the pure kaolin clay (169.4 kPa) prepared under the same condition. This can be explained by the low clay fraction in the soil compared to the S50K50 mixture. However, the friction angle of S75K25 is higher than that of S50K50 and the pure kaolin clay (13.8°) due to the sand fraction in the mixture. All the results are in good agreement with the literature.

3.2 *Influence of traffic cycles on soil surface degradation*

3.2.1 *Eroded masses collected at the soil surface*

Figure 5 shows the masses of eroded soil collected at the surface of compacted specimens after 10 000 traffic cycles. Test results correspond to I', II and III compaction configurations.

Note that, for practical reasons, the traffic cycles for the specimens prepared in the configuration I were stopped after 100 cycles. In fact, the high soil humidity generates an important settlement of the soil under traffic cycles. The eroded masses could not be measured for this configuration.

From Figure 5, it can be observed that the studied soils have a lower degradation potential in configuration II, compared to the other configurations. However, important surface degradation is observed for configurations I' and III. For S50K50, the soil surface degradation potential is higher for configuration I' compared to configuration III, while for S75K25, the soil surface is slightly more degradable for configuration III compared to configuration I'.

At the same hydric state and dry unit weight, for configurations I' and II, prepared on different paths, the soils have a high degradation potential for configuration I' compared to configuration II. The drying process for I' seems to increase the soil degradation potential at the surface. However, the low degradation observed in configuration II is linked to the over-compaction of the soil at this point.

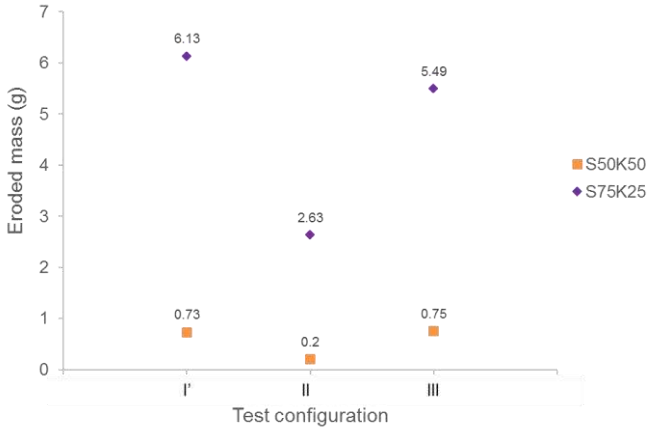

Figure 5. Influence of traffic cycles on compacted soil surface degradation.

The effect of compactness is well underlined. The eroded mass for configuration III is 2 to 4 times higher than for configuration II. The over-compaction of the soil for configuration II allows a better soil densification, and therefore improves the stability at the surface.

The soil surface behaviour under traffic cycles is intimately related to the soil type. The soil surface degradation of S75K25 is 7, 8 and 13 times greater than for S50K50 for III, I' and II configurations, respectively. Degradation is proportional to the granular fraction in the soil (i.e. disproportional to soil cohesion) due to the friction potential of the soil (Fig. 4). Soils with a large fine fraction are less susceptible to degradation because the fine fraction imparts cohesion to the soil as seen in the previous section (Fig. 4), which decreases degradation potential of the soil.

3.2.2 *Grain size distributions*

The grain size distributions of the eroded soil are compared with those of unconsolidated and dry soil noted as "intact". The comparison results are shown in Figures 6(a) and 6(b) for S50K50 and S75K25, respectively.

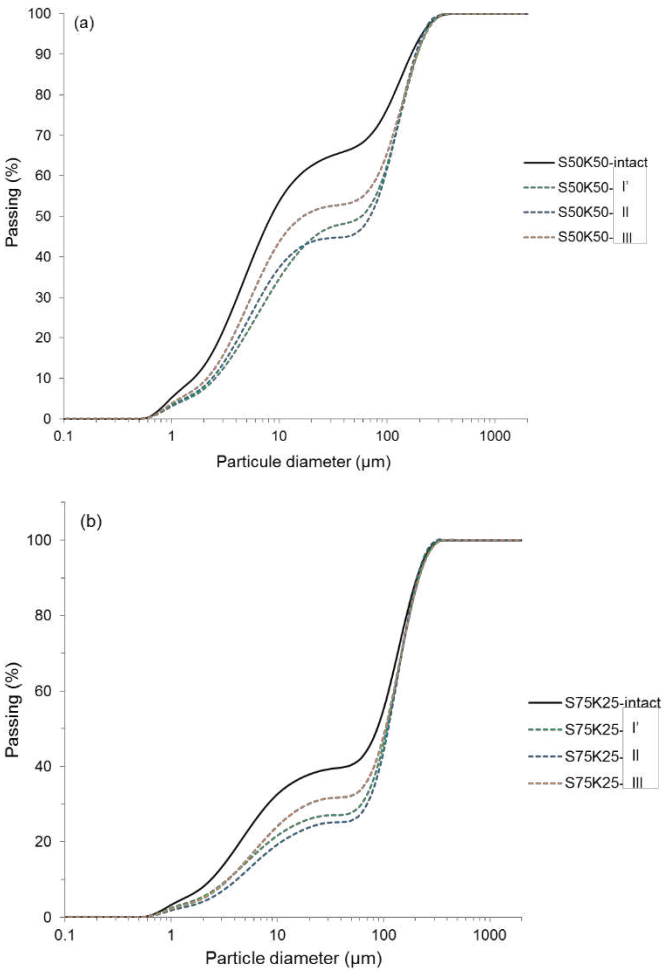

Figure 6. Influence of traffic cycles on grain size distribution of soil (a) S50K50, (b) S75K25.

The grain size distributions of the eroded soil show that the traffic cycles generate aggregate of soil particles coarser than in the intact soil for all tested configurations. This phenomenon can be related to the detachment of soil aggregates formed after moistening and merged during compaction. Scanning Electronic Microscopy observations of eroded soil, shown in Figure 7, confirm these statements. Figure 7 shows that the eroded soil collected from the surface is composed by soil aggregates of different sizes. The sand grains covered by the clay particles, and/or only by clay particles form these aggregates.

It may also be noted that the size of the eroded aggregates at I' is relatively close to that of the eroded aggregates at II, and smaller size, close to the intact soil is observed for the specimen compacted at III.

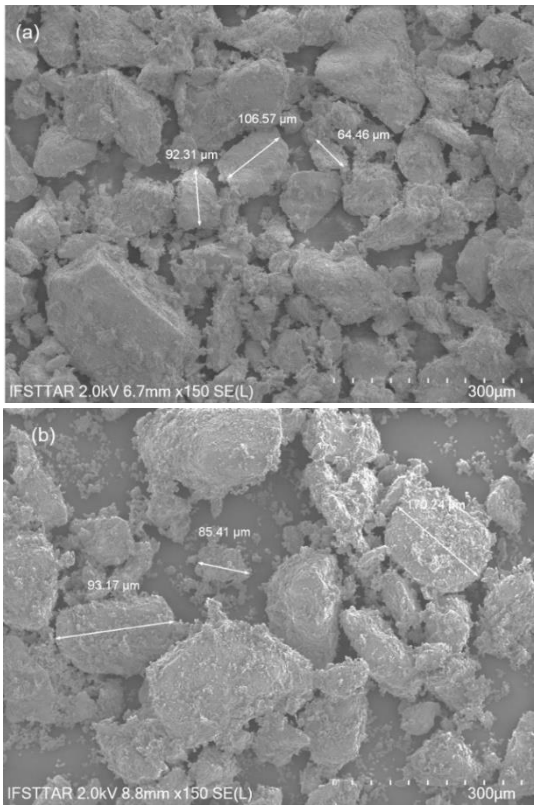

Figure 7. SEM observations of eroded soil at the surface specimens compacted at configuration 'III' (a) S50K50, (b) S75K25.

3.3 *Influence of traffic cycles on pore size distribution of soil*

The influence of traffic cycles on the soil microstructure of compacted soils was also analysed. Comparison was made between PSD measured with non-degraded (ND) and degraded (D) soils, for each configuration tested. PSD are plotted in Figures 8(a) and 8(b) for S50K50 and S75K25, respectively.

S50K50 has a monomodal distribution at SPO configurations with a micropore diameter of 0.1 µm, while a multimodal distribution is observed for the soils submitted to traffic cycles under configurations II and III. The size of the macro-pores is between 0.4 µm and 1.6 µm.

For S75K25, two sizes of macro-pores are underlined, one with a size of about 1 µm diameter for configurations I-ND and I'-D, and the second with values between 9 µm and 13 µm for all configurations, except I'-D. However, the size of the micropores remains unchanged and equal to 0.1 µm whatever the tested configuration, for both studied soils. Based on these results, it can be concluded that the micropore size is developed during soil moistening and less impacted by compaction.

The influence of the compaction implementation is noticed by comparison between results obtained with configurations I, II and III, before traffic cycles. PSD results show large macro-pore sizes for configurations II and III compared to I. Macro-pores intensity takes low values for I, near zero for S50K50, middle values for II and highest values for III. This phenomenon can be explained by the heterogeneous distribution of water in the soil during compaction. The availability of the water in the soil in configuration I results in a significant decrease in the macro-pores size. The mechanism can be explained, partly, as follows: the water, present in the soil plays the role of a lubricant, fills the voids between soil particles, bringing them closer, and sometimes merge all of them to form a plastic aggregate, that deforms under compaction effort. If the quantity of water is not sufficient to fill the void space, then, less aggregates are formed, and the modification of PSD is governed by compaction. The latter is observed in the case of configurations II and III.

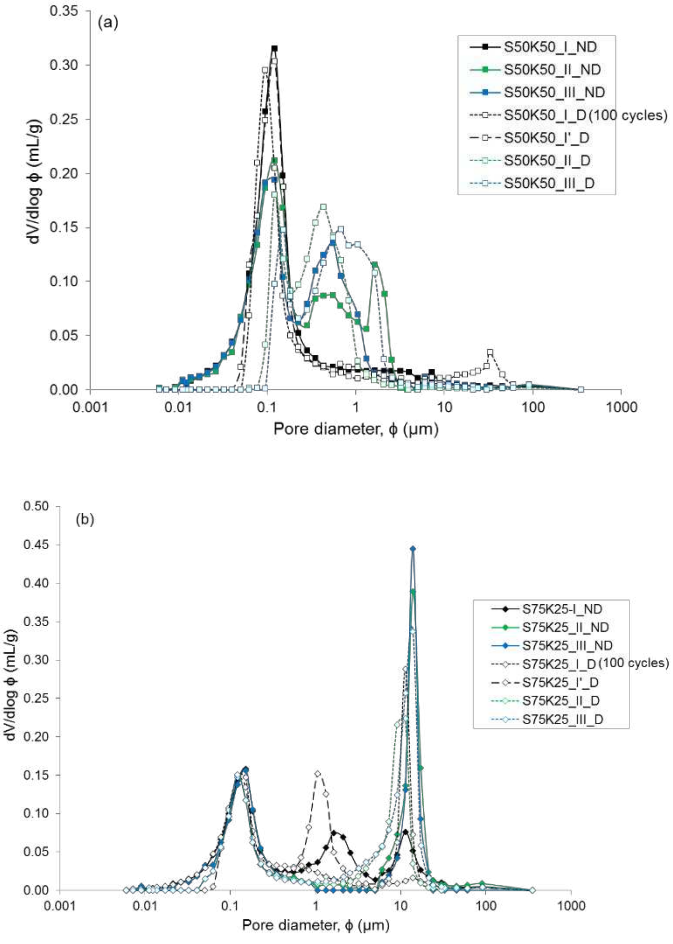

Figure 8. Influence of traffic cycles on pore size distribution of soil not degraded (ND) and degraded (D): (a) S50K50; (b) S75K25.

The effect of traffic cycles on soil degradation can also be observed. Figure 8 shows that the cumulative effect of the traffic cycles leads to a decrease in macro-pores except for S75K25-I, where the high soil moisture occurs to generate an increase in macro-pore size. An open soil structure is observed after traffic.

The combined effect of drying and traffic cycles is studied. PSD results demonstrate that the combination of compaction and traffic cycles (I) generate more reduction of the macro-pore size compared to the combination of compaction, drying and traffic cycles (I'). Based on these findings, the effect of drying on the reduction of the macro-pore size is considered to be less significant.

4 CONCLUSIONS

The combined effect of traffic cycles and hydric state on the surface erosion of compacted soils is analysed in this study. Experiments involve soil surface erosion and the change of the microstructure of soils under different implementation configurations. Soil compaction and traffic cycles were carried out by means of a laboratory roller compactor, and a laboratory traffic simulator. The tests are performed on two different soils composed by mixtures of Speswhite kaolin clay and Hostun sand.

Based on test results, the following conclusions can be noted:

- Test results show that low eroded soil quantity is measured under implementation configuration II compared to I and III. With similar hydric state, the configuration I' presents more eroded soil particles than the configuration II.
- The quantity of eroded soil occurs to be proportional to the coarse fraction in the soil. Soils with a large fine fraction seem to be less degradable due to higher soil cohesion. The results are in good agreement with results of shear tests in terms of friction angle and cohesion.
- The grain size distributions of the eroded soil show that traffic cycles remove soil aggregates coarser than those of the intact soil. Grain size distribution of the eroded soil is in good agreement with SEM observations.
- The size of the macro-pores is significantly reduced by compaction and traffic cycles compared to that obtained by a combination of compaction drying prior traffic cycles. Micropore size remains unchanged for all configuration tested.

Based on the previous results, to reduce the erosion of unpaved road surface due to traffic, the compaction configuration corresponding to the configuration II appears to be the most convenient. However, the long-term behaviour of the soil compacted in this configuration, and the dust emission potential of the soil have yet to be investigated.

5 ACKNOWLEDGEMENTS

The authors would like to express their gratitude to: Fédération Nationale des Travaux Publics (FNTP), Syndicat Professionnel des Terrassiers de France (SPTF) and VINCI Constructions Terrassement (VCT) for their financial support, Prabhu Chandan and Surabhi Bhuyan, from National Institute of Technology, Rourkela, for their valuable contribution to this research during their internship.

6 REFERENCES

Addo, J.Q. & Sanders, T.G. 1995. Effectiveness and environmental impact of road dust suppressants. MPC Rep. No. 92-28A, *Mountain Plains Consortium*.

Bolander, P & Yamada, A. 1999. Dust palliative selection and application guide.

Boulter, P.G. 2005. A Review of Emission Factors and Models for Road Vehicle Non-Exhaust Particulate Matter. *Published Project Report PPR065*. TRL Limited.

Edvardsson, K. & Magnusson, R. 2009. Monitoring of dust emission on gravel roads: Development of a mobile methodology and examination of horizontal diffusion. *Atmospheric Environment* 43: 889-896.

Etymezian, V., Kuhns, H., Gillies, J.A., Green, M., Pitchford, M. & Watson, J. 2003. Vehicle-based road dust emission measurement: I- methods and calibration. *Atmospheric Environnement* 37: 4559-4571.

Foley, G., Cropley, S. & Giummarra, G. 1996. Road Dust control techniques: evaluation of chemical dust suppressants performance Australia. ARRB Transport Research Ltd Vermont South, Victoria: 54. 143p.

Han, B. Bai, Z., Guo, G., Wang, F., Li, F., Liu, Q., Ji, Y., Li, X. & Hu, Y. 2009. Characterization of PM10 fraction of road dust for polycyclic aromatic hydrocarbons (PAHs) from Anshan, China. *Journal of Hazardous Materials* 170: 934-940.

Lohnes, R.A. & Coree, B. J. 2002. Determination and evaluation of alternate methods for managing and controlling highway-related dust. *Iowa Highway Research Board Report.*

Moosmuller, H., Varma, R., Arnott, P.W., Kuhns, H.D., Etyemezian, V. & Gillies, J.A. 2005. Scattering cross-section emission factors for visibility and radiative transfer applications: military vehicles traveling on unpaved roads. *Journal of the Air & Waste Management Association* 55: 1743–1750.

Moses, T. Eckoff, T. Connor, B. & Perkins, R.A. 2012. Construction Dust Amelioration Techniques. Alaska Department of Transportation & Public Facilities.

Succarieh. M. 1992. Control of dust emissions from unpaved roads. Report prepared for Alaska cooperative transportation and Public facilities research program.

Thenoux. G. Bellolio. J.P. & Halles, F. 2007. Development of a Methodology for Measurement of Vehicle Dust Generation on Unpaved Roads. *Journal of the Transportation Research Board: Transportation Research Board of the National Academies*, Washington, D.C. 1989(1): 299-304.

Vinkovic, I. 2005. Dispersion et mélanges turbulents de particules solides et de gouttelettes par une simulation des grandes échelles et une modélisation stochastique lagrangienne, application à la pollution de l'atmosphère. PhD Thesis. *Ecole centrale de Lyon*.